



# Active–passive combined energy-efficient retrofit of rural residence with non-benchmarked construction: A case study in Shandong province, China<sup>☆</sup>



Xinyi Hu<sup>a</sup>, Yiming Xiang<sup>b</sup>, Hong Zhang<sup>a,\*</sup>, Qi Lin<sup>c</sup>, Wei Wang<sup>a</sup>, Haining Wang<sup>d,e</sup>

<sup>a</sup> Department of Building Technology and Science, School of Architecture, Southeast University, Nanjing 210096, China

<sup>b</sup> Bartlett School of Construction and Project Management, University College London, London WC1E 7HB, UK

<sup>c</sup> Graduate School of Architecture, Planning and Preservation, Columbia University, NY 10027, USA

<sup>d</sup> State Key Laboratory of Green Building in Western China, XI AN University of Architecture and Technology, Xi'an 710055, China

<sup>e</sup> School of Architecture, Southeast University, Nanjing 210096, China

## ARTICLE INFO

### Article history:

Received 19 October 2020

Received in revised form 18 January 2021

Accepted 17 February 2021

Available online xxxx

### Keywords:

Chinese rural residence

Energy-efficient retrofit

Wall selection

Rooftop photovoltaic system

## ABSTRACT

Unlike standard-restricted and well-equipped urban residential buildings, a large portion of rural buildings sacrifice indoor comfort and energy efficiency to reduce the initial investment. Therefore, cost-effective retrofit strategies for rural buildings are urgently needed to better living conditions and create higher energy efficiency. This study developed a framework to choose the optimal economical retrofitting strategies for existing rural buildings by taking both active and passive approaches into consideration. The building retrofitting measurements were a combination of thermal performance improvement for external walls and a solar photovoltaic generation system for the rooftop. With the case of a rural dwelling in Shandong province, this study first assessed the thermal transmittance of the external walls and collected geometry and operational schedules to create a building model for the later energy simulation. Environmental monitoring was also conducted for two months – in February for winter and August for summer – to obtain actual indoor temperatures, which were used to calibrate the energy model within a 10% error rate. In total, 17 retrofitting plans were then set up and analyzed in this study. The results showed that when applying the cost-optimal retrofit plan, there is the great potential to reduce energy use by 20.5% and to balance the annual building energy consumption with a payback period of 10.7 years. Finally, the proposed framework was proven to be accurate and feasible and was expected to be widely used in the improvement of living conditions in Chinese rural areas.

© 2021 The Author(s). Published by Elsevier Ltd. This is an open access article under the CC BY-NC-ND license (<http://creativecommons.org/licenses/by-nc-nd/4.0/>).

## 1. Introduction

As reported in 2019, the built-up area in China had increased to 64.3 billion m<sup>2</sup>, where residential buildings account for 71%, consuming 62% of the natural energy supply (China Building Energy Consumption Report 2019, 2019). Considering the large number of existing stock and the high cost of demolition and reconstruction, it is more technically feasible and financially effective to retrofit than to build. Meanwhile, debates concerning environmental upheaval and energy usage highlight the urgent need

for more sustainable development in the building sector. With the implementation of “top-to-bottom” energy-efficient renovation programs targeting urban residential buildings in northern China from 2007 to 2010, around 0.19 billion m<sup>2</sup> buildings were retrofitted, with the energy intensity reduced by 20% (Bao et al., 2012). The energy consumption of urban residential buildings in 2017 was 11.84 kg of coal per square meter of building area (kg ce/m<sup>2</sup>) (China Building Energy Consumption Report 2019, 2019). However, rural dwellings, accounting for 41.7% of total residential buildings, are facing huge energy challenges, as 80% have no insulation for building envelopes (Song and Deng, 2018). A high percentage of rural dwellings sacrifice indoor comfort and energy efficiency during construction to reduce the cost, and rural residents are paying a large sum for extra heating, health, and environmental resources because of uncomfortable indoor spaces (Qi et al., 2019). Therefore, there is a necessary and urgent need for cost-efficient retrofitting to improve living conditions and the comfort of rural dwellings.

<sup>☆</sup> Acknowledgments: This research was funded by the National Natural Science Foundation of China (51778119) and Open fund projects of State Key Laboratory of Green Building in Western China (LSKF202020).

\* Correspondence to: Southeast University, School of Architecture, Department of Building Technology and Science, Nanjing, Jiangsu Province 210096, China.

E-mail address: [seu\\_zheng\\_studio@sina.com](mailto:seu_zheng_studio@sina.com) (H. Zhang).

However, the vast majority of early rural houses were built by local labor based on experience rather than construction codes. Compared to standard-restricted urban residences, the construction methods and materials used in rural construction vary greatly from region to region and from construction era to construction era. Considering the retrofit scale, cost, and practical implementation capacity in rural areas, it is unreasonable to merely replicate the retrofit methods that are being implemented in old urban communities nowadays (Evans et al., 2014). Therefore, case demonstrations are needed to illustrate how to carry out energy-efficient retrofitting of Chinese rural houses under previous non-benchmarked construction.

### 1.1. Passive and active building-energy retrofit

Literature on building energy-efficiency refurbishment mainly focused on passive or active approaches, namely the energy-demand side. The widely used passive energy-saving method minimizes the energy lost through the envelope by reducing thermal conductivity and improving airtightness, decreasing the excessive energy demand (Suárez and Fernández-Agüera, 2015). According to Magrini's research (Magrini et al., 2014), the thickness of the insulation layer has a reasonable limit, which means that the thickness cannot be increased blindly or the moisture transmission inside the wall would be affected. Nevertheless, not all envelope retrofit methods are feasible. They are frequently limited by economic factors or technical factors and, therefore, need to be evaluated cautiously. For instance, in the case of the affordable building reconstruction mentioned in Casquero-Modrego and Goñi Modrego (2019), given the series of problems described and the solutions proposed from the envelope to the structure, only insulation material was added to the opaque envelope part instead of implementing all the methods put forward, owing to limited government funds and the huge number of buildings that are in urgent need of renovation.

The other way of building retrofit is known as active energy-efficient strategies, including the application of upgraded HVAC systems (Xin et al., 2018) and the replacement of high-energy appliances (Gupta and Gregg, 2016), which can efficiently decrease the energy use to a certain extent (Luddeni et al., 2018). Asaee et al. (2017) estimated that 36% of energy consumption could be reduced if air-to-water heat pump retrofitting were conducted nationwide in Canada. Hinnells (2008) declared that there is a potential of 75%–90% reduction in lighting energy consumption compared to conventional patterns with a combination of daylight sensors, energy-efficient lighting, and lighting control.

### 1.2. Active–passive combined building-energy retrofit

To achieve more significant energy savings, both active and passive approaches are often adopted in one retrofit project, improving the energy performance of envelope components and equipment systems simultaneously. Liu et al. (2018) assessed a holistic strategy with building envelope, heating system, and outdoor heating-pipe networks, and it had the potential for reducing electricity consumption of a high-rise residential building in Beijing in winter and summer by 34% and 11%, respectively. Mata et al. (2013) found that the combination of various retrofit methods, including wall insulation, window replacement, and recovery system improvement, could achieve 53% reduction of energy demand in Swedish residential buildings.

Coupled with the requirements of the Kyoto Protocol's Clean Development Mechanism (CDM) (Zhou et al., 2013), various renewable energy technologies have been employed in many retrofit programs in recent years combined with mature energy-efficiency methods. In a study by Nihal et al. (2018), the results

indicated that, after separate calculation, the combination of wall, window, and roof insulation and the installation of a solar domestic hot water heater system respectively resulted in 50% and 55% energy savings, and the simultaneous use of them was considered the optimal energy retrofit strategy for an existing single-family home in Turkey. Becchio et al. (2015) presented a guideline for designing retrofit plans combining high-efficiency building envelopes, technical systems, and solar photovoltaic systems, transforming a high-performing single-family house to a nearly zero-energy building. The above-mentioned studies illustrate the large amount of energy-efficient methods that can be applied to retrofitting residential buildings. However, the feasibility of these comprehensive methods applied in rural circumstances needs to be further identified according to the local climate, resource availability, economic level, and other conditions.

### 1.3. Model calibration for building energy retrofit

Measurement and simulation are frequently employed as efficient ways to assess the potentials of various energy-saving methods before initiating a refurbishment program for existing buildings (Hong et al., 2014). An energy model is traditionally established to conduct simulations with the application of building energy simulation programs (Augenbroe, 2002), such as Energy-Plus and TRYNS. In current cases, it is very common for users to apply existing well-established templates or representative constructions in the parameter input procedure (Coakley et al., 2014). Such simplified methods may save time in the early design stage but would consequently further widen the gap between the simulated and actual values, especially for accurate retrofit projects (Li et al., 2015).

On-site surveys are conducted for calibrating the simulation model, minimizing the discrepancy between simulated energy use and observed data (Manke et al., 1996), which is considered the fundamental step of building energy simulation (Ayres and Stamper, 1995). Numerous calibration approaches based on iterative parameter tuning manually have been developed, including collecting supplemental evidence (Pan et al., 2007) and applying graphical comparisons (Pedrini et al., 2002). These manual calibration methods combine expertise and physical situations in a trial-and-error process, leading to a more reliable energy model (Coakley et al., 2014). In order to optimize the aforementioned time-consuming and costly process, auto-calibration is further developed based on mathematical and statistical knowledge, converting part of the manual adjustments into an automatic process, which obviously enhances the efficiency of model calibration (Yang et al., 2016).

This research about energy simulation models has been conducted for several decades. But for Chinese rural houses that were built without reference to construction standards, relying on the experience and "creativity" of local workers, more in-depth research is needed. What actual data is needed and how to obtain it from field measurements and user surveys requires specified illustration. The data is used to build energy models that are more in line with reality. If the gap between the simulation results and the actual situation were reduced to within the acceptable deviation through calibration by energy consumption bills (Chen et al., 2013) or indoor temperature (Taheri et al.), only then could the energy model be employed for the following evaluation and selection of different energy-conservation methods.

### 1.4. Optimization model for energy-efficient retrofit

When multiple components are to be modified in one refurbishment project, the best combination of retrofit selections should be identified according to project orientation with the

application of an optimization model. The optimization objectives can be roughly divided into two categories, economic and environmental, which are often conflicting (Rosso et al., 2020).

Tahsildooost and Zomorodian (2020) presented a tool for selecting the optimum retrofit action combination for the envelope of rural houses in different climates with the objectives of minimum energy consumption, carbon emission, and retrofit cost. However, the retrofit objects were simplified as arithmetic parameters instead of considering the actual materials. Fan and Xia (2017) established a multi-objective optimization framework for envelope retrofit and rooftop PV system installation. A genetic algorithm (GA) was applied to find the optimal strategy with minimum energy consumption and payback period and maximum net present value under the different retrofit budget constraints. Ascione et al. (2019) proposed a simulation-based performance optimization model with EnergyPlus for simulation and GA for optimization. In total, nine design variables were taken into account during the optimization process and a nearly zero energy optimal strategy and a cost-optimal strategy were determined under multiple criteria. Most of the previous optimization models used idealized numerical calculations. A uniform range of values and idealized iso-difference intervals were incorporated into the calculation, neglecting the relevant technical and construction limitations occurring in practical applications.

### 1.5. Problem statement

The design and construction of Chinese rural residences vary across provinces because of the diverse cultural and geographical features, economic levels, and resource availability. Residences are usually one or two floors, mostly with courtyards (Yang et al., 2010). Common structures are masonry structure, reinforced concrete frame structure, as well as wood structure, stone-wood structure, adobe, and rammed earth structure and other traditional structures. The proportion of masonry structures and reinforced concrete structures is positively related to the income level of local farmers (Li et al., 2011). Roofs and floors are basically made of hard cement without insulation. 80% of the external walls are made of solid clay bricks with poor thermal performance, which has been banned in construction in China since 2011 (Li et al., 2020). There are also walls made of hollow bricks. Most windows are single-layered glass with wooden, steel, or aluminum frames (He et al., 2014).

Different from urban residential buildings, rural houses are mostly built without the governance of uniform construction codes. Instead, they are built by local builders based on their experience and locally available materials without prior formal, detailed construction drawings. Therefore, there is a great deal of particularity in the construction of rural houses, most of which do not adhere to specific construction practices or consider thermal properties. As a result, thermal performance of these self-built houses is hard to guarantee. This also results in difficulties simulating the current thermal situation of these houses, which very little literature has studied. However, in the energy-efficient retrofit process of a rural house, reducing the error between the energy model and the reality to an acceptable range is a necessary prerequisite for the subsequent simulation of retrofit methods.

The energy structure in rural areas is greatly influenced by the characteristics of village layout and living standards of local farmers. In China, rural villages usually have low building density, most of which are out of the national district heating area. Except electricity and fossil fuels, traditional biomass energy, including firewood, dry weed, and other agricultural residues, is the dominant fuel in the rural energy structure (Evans et al., 2014). Traditional biomass is cheap, but directly burning it inside homes can cause severe indoor air pollution, which can have a negative

impact on occupant health (Yang et al., 2010). Therefore, there is a need to improve the rural energy structure. In accordance with local resource availability, it is recommended to promote small-scale, decentralized energy systems in rural areas, especially the application of renewable energy sources, such as biomass and solar energy (Zhang et al., 2009).

In this study, one self-built rural house in Shandong province was selected as the case building. It possesses the features of a common layout, a moderate building scale, and a non-benchmarked but mature construction method that can effectively represent the general situation of rural houses in the local area. Detailed description is elaborated upon in Section 2.1. The energy-efficient retrofit methods of the case house mainly consider adding insulation material to the external walls to reduce the extra heat loss and installing a rooftop PV system to reduce the dependence on the power grid. Most Chinese rural houses are facing a shortage of envelope insulation. It is reported that only 3% of rural houses in southern regions and 11% of those in the north have high-quality insulation (Yang et al., 2010). Among all the envelope components, external walls, with the largest area ratio and higher energy-saving potential, hold the improvement priority in both application frequency and energy savings, followed by the windows and roof (Liu and Guo, 2013). In addition, compared to the replacement of windows and the addition of an insulation layer to the pitched roof, the installation of external insulation on the external walls has the least impact on indoor occupant life. Considering the low density of rural housing and their idle roofs, coupled with Shandong province's abundant solar resources, the promotion of small-scale decentralized solar systems, such as rooftop PV systems, in rural areas of Shandong province is suitable.

Therefore, this study seeks to answer the following questions:

(1) What data should be collected through on-site measurement and user survey to establish an energy model for non-benchmarked rural houses with an acceptable error rate between the simulation results and the reality?

(2) How can an optimization model be formulated under actual construction constraints to select the optimal environmental and economic combination of wall retrofit and rooftop PV system installation?

Due to geographic diversity, economic capacity, and local resource availability, rural houses in different parts of China are generally energy inefficient and their energy performance varies greatly by the effect of their non-benchmarked construction. To improve the comfort and living conditions of rural dwellers and to narrow the energy gap and inequality between urban and rural areas, energy-efficient retrofitting of these houses is therefore urgently needed. This study is expected to provide a demonstration for other self-built rural houses with poor energy performance of an efficient and feasible retrofit.

## 2. Methodology

The methodology applied in this paper is a four-step procedure: (i) an energy simulation model was created by Design-Builder software with input parameters collected from field measurements and user survey; (ii) monitored temperature data and actual electricity bills were applied to calibrate the energy model; (iii) retrofit option sets with both envelope retrofit options and different numbers of rooftop PV panels were generated according to the actual construction conditions; (iv) a calibrated energy model was applied to simulate the energy savings of retrofit option sets and the most economically optimal one that satisfied the annual energy consumption balance was selected through the optimization model.



**Fig. 1.** The geometry model in the SketchUp program (left) and the real profile of case rural building (right).

## 2.1. Case study

As shown in Fig. 1, the selected building is a one-story, reinforced concrete-structured building, located in the countryside of Jining, Shandong province, China. According to records ([China Weather Network, 2009](#)), it is a city in cold climate region, represented by distinguished seasons and an alternation of wet and dry weather. The range of annual average temperature ( $-1.7^{\circ}\text{C}$  in January and  $26.8^{\circ}\text{C}$  in July) and daily average temperature (approximately  $11^{\circ}\text{C}$ ) leads to a complex demand on its air-conditioning systems. Both heating and cooling systems are necessary. 25% (441.74 mm) of precipitation happened in summer, and only 4% (27.8 mm) was measured in winter. The annual average solar radiation hour is 2272.3 h/year, which creates an ideal environment for PV application.

The case building was constructed in 2017 and consists of four bedrooms, one dining room, one living room, two bathrooms, and one kitchen. This dwelling is a typical case of a rural house because of the special construction methods and local materials it applied. The information about architecture design and construction detail was obtained through drawings provided by the contractor. Local agricultural waste straw was mixed with foamed concrete as wall filler by the local construction workers. Steel cages were used as the container for the mixed filler and the base of the sprayed concrete, which were combined with the structural columns to form the special composite wall. There was no insulation layer on the external walls or the roof. Fig. 2 shows the details of the design and construction of the current ground floor, external walls and the roof. Here is a brief description of them: Triangular trusses were built into the pitched roof. There were no insulation materials installed on the roof or ceiling, but the closed cavity that formed between them became a temperature buffer. Apart from a decorative painting and waterproofing membrane, no insulation material was attached to the surface of external walls. Concerning the heated floor, soil was first solidified to the design elevation ( $-190\text{ mm}$ ); a 100 mm reinforced-concrete layer then formed the surface of the structure with 30 mm insulation material and heating pipes installed above that. As for the glazing system, a double-deck broken bridge aluminum alloy window was the only form of it, with a U-value of  $2.75\text{ W/m}^2\text{ K}$ .

The air-conditioning operational in the building consists of two parts: (1) heated floor with air-source heat pump for the heating system and hot water system, rather than using coal or other fuel in winter and (2) split air conditioners for the cooling system in summer. The lighting system, a LED light source in each room, were fully manually controlled. In addition to heating and cooling, the remaining consumption is  $20.8\text{ kWh}/(\text{m}^2\text{ year})$ . The major characteristics of the case building are listed in Table 1.

## 2.2. Building energy model and calibration

With the use of DesignBuilder, an EnergyPlus engine-based energy simulator, a 3D energy model was created based on existing

**Table 1**

Major characteristics of selected building.

Location	Jining, China $35^{\circ}57' - 34^{\circ}36' \text{N}$ , $117^{\circ}36' - 115^{\circ}52' \text{E}$	
Gross area	$126.2\text{ m}^2$	
Construction	Reinforced concrete structure, composite walls, pitched roof	
Window	$6+25A+4$ (aluminum window frame without break) $17.48\text{ m}^2$ (glazing area)	
HVAC system	Heating Cooling	Air-source heat pump with heated floor 1 split air conditioner in the living room

characteristics of the case building, the input parameters of which were collected from various resources.

**Geometry** Building drawings and other relevant documents were collected from the original construction team, and the surrounding environment was measured through field study. This information was used for the generation of the simulation energy model.

**Building construction details:** The thermal transmittance of the external wall was assessed based on a heat flow meter method during the coldest month, considering the particularity of its structure and material. The proper measurement dots were first confirmed using an infrared camera. As shown in Fig. 3, there was significant temperature difference between the foamed concrete part and the structural column in the winter, which was  $3.3^{\circ}\text{C}$  and  $1.6^{\circ}\text{C}$  on the inside and outside of the external wall, respectively. In order to avoid the effect of direct sunlight, the western wall, obscured by the adjacent building, was selected as the measuring object. The heat flow meters and temperature sensors were placed on the surface of the foam concrete part and the structural column (considered the thermal bridges) for 96 h of continuous detection (Fig. 4). The thermal transmittance of the thermal bridges and composite wall obtained in the in-situ measurement were  $2.915\text{ W/m}^2\text{ K}$  and  $0.912\text{ W/m}^2\text{ K}$ , respectively. The other components of the residence, including the roof, floor, and glazing parts, adopted a conventional construction method described in Section 2.1, and the materials, modeling, and simulation were based on the working drawings.

**Operation schedule:** The HVAC system of the case house consists of an air-source heat pump with heated floor in all rooms except the bathrooms and kitchen and a split air conditioner only in the living room (see Table 2). The operation period of the HVAC system for winter is November 15th to the following March 15th and for summer June 16th to September 8th. The natural ventilation schedule and occupancy density were obtained from the user survey.

To calibrate the simulated energy use, the actual monthly energy uses for year 2019 obtained from electricity bills, as well as the temperature data of the monitored rooms, were used for comparison. The temperature of monitored rooms in the case building were collected in the winter (from February 1st to

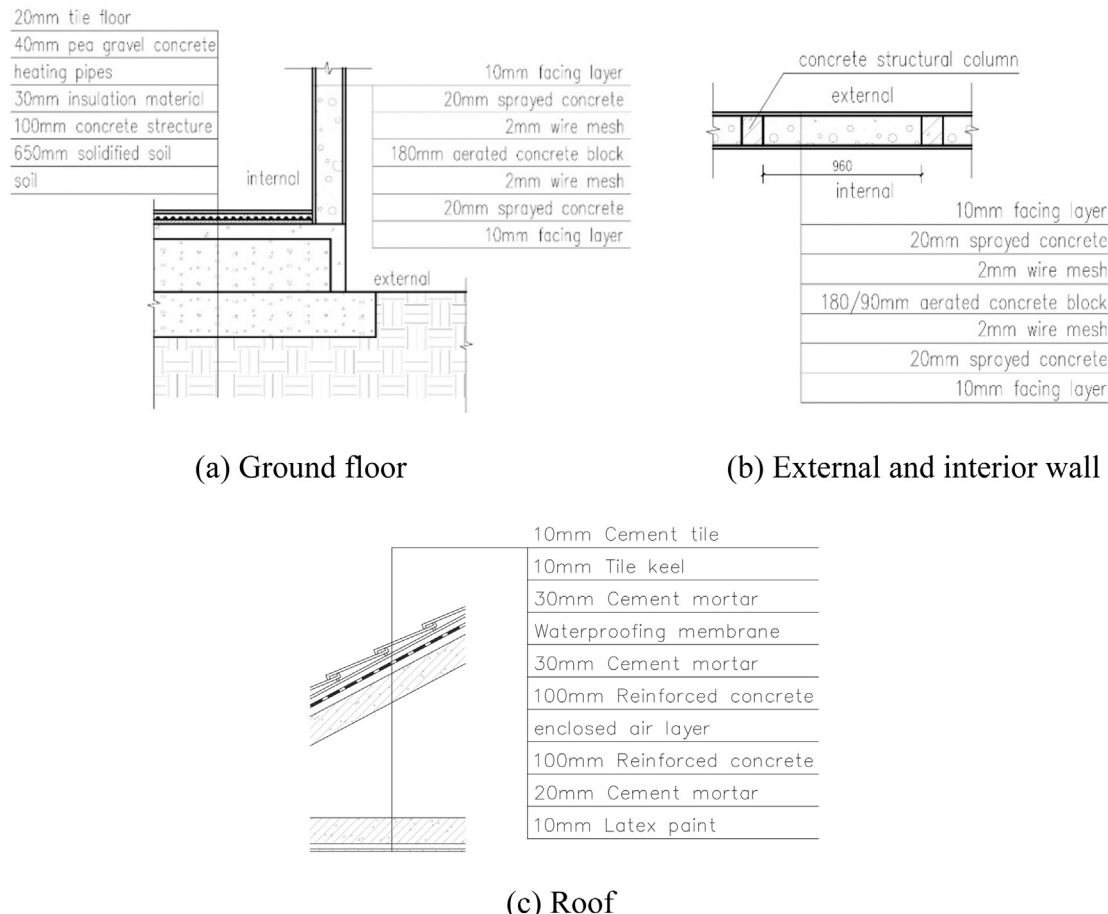


**Fig. 2.** The construction details of the existing ground floor (a), wall (b), and roof (c).

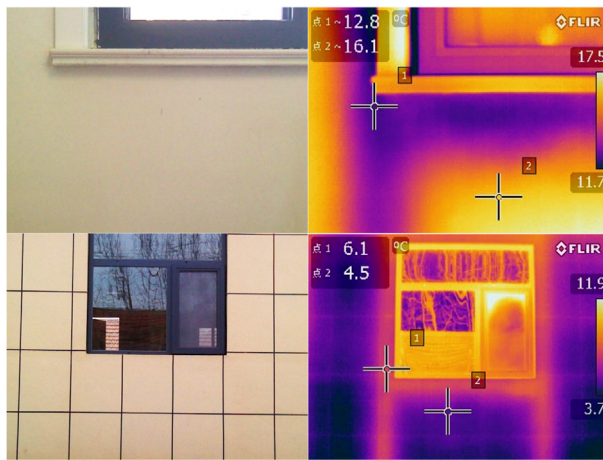


**Fig. 3.** Thermograms: inside (top) and outside (bottom) of external walls.

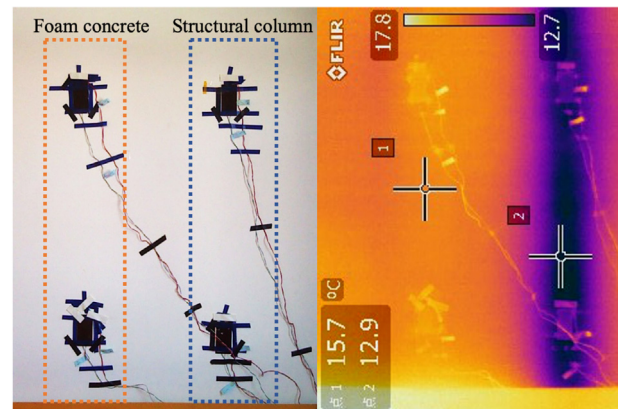


**Fig. 4.** Sensors for thermal transmittance measurement.

February 28th, 2019) and summer (from August 13th to September 12th, 2019), which were automatically recorded and transmitted via wireless to the database by the sensors from the MI corporation. Fig. 5 gives information on the sensor distribution for temperature monitoring and thermal transmittance measurement.

Fig. 6 presents a comparison of outdoor and indoor temperatures during a typical week in winter. It was observed that the highest average indoor temperature was in the living room facing

**Table 2**  
Operation characteristics of the case building.

HVAC	Heating	Cooling
Setpoint temperature	18.5 °C	24 °C
System coefficient	4.0	3.9
Occupancy		
Occupancy density	0.048 people/m <sup>2</sup>	
Metabolic factor	0.88	

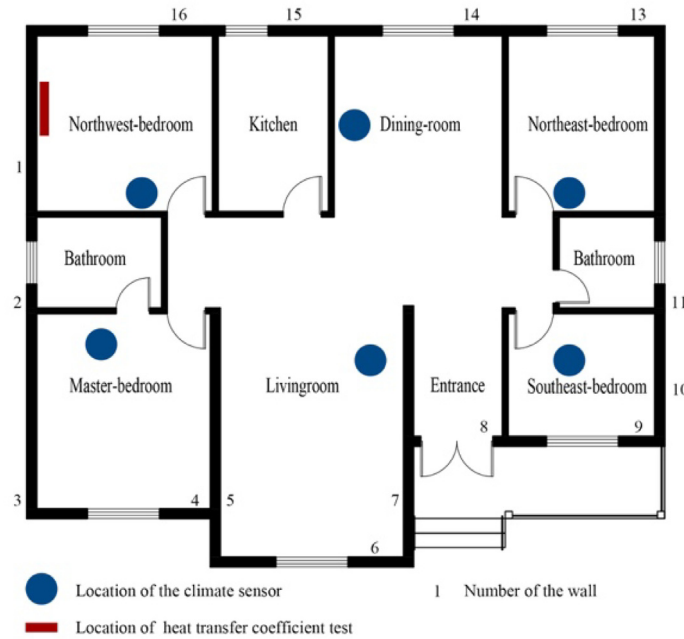


**Fig. 5.** The distribution of environment sensor installations and the measurement location of heat transfer coefficient of the external wall.

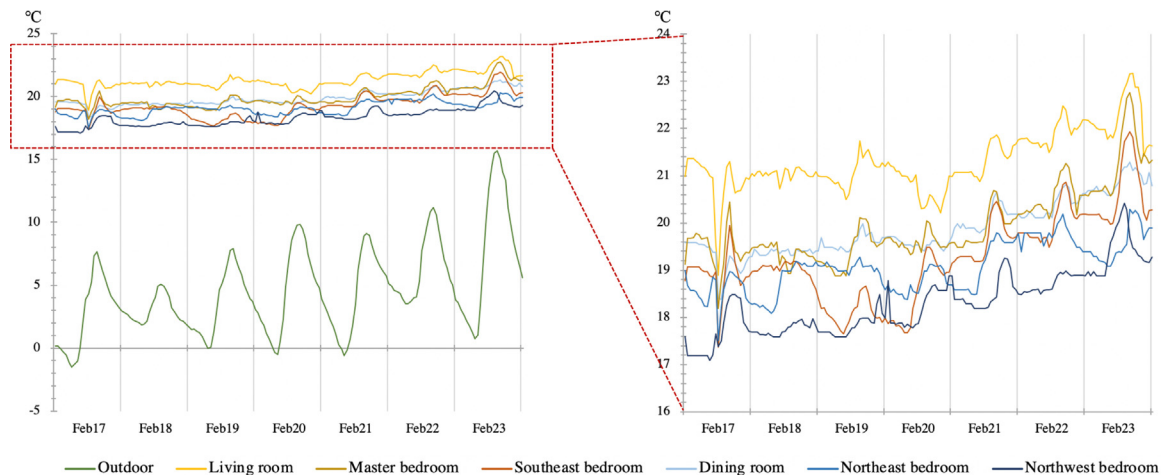


**Fig. 6.** The results of outdoor and indoor temperature measurement during a typical week in winter.

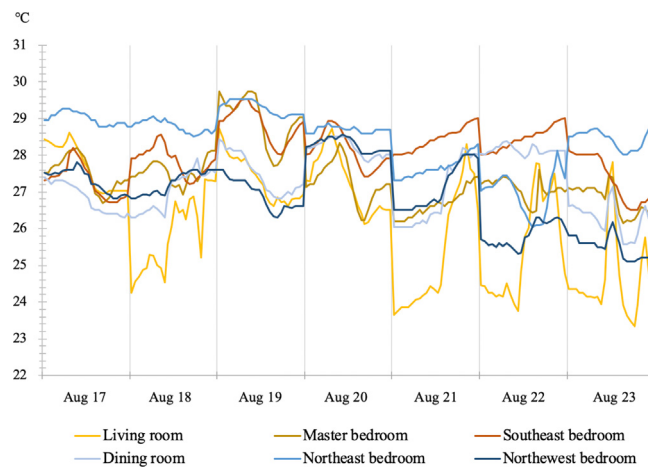
south ( $21.3^{\circ}\text{C}$ ), while the dining room and master bedroom shared the same average temperature ( $19.9^{\circ}\text{C}$ ), higher than the two northern bedrooms. The daily indoor temperature differences increased as the daily outdoor temperature difference was greater. Furthermore, the daily indoor temperature differences in the rooms facing south were greater than those of the rooms facing north, and the maximum indoor temperature in the south-facing rooms occurred between 15:00 and 16:00 every day. The dining room is connected to the living room through a corridor, without any doors between them, but the daily temperature difference in the south-facing living room was significantly higher than the north-facing dining room.

Fig. 7 illustrates the indoor temperature of each room during a typical week in summer. The house is equipped with a split air-conditioning in the living room while the other rooms have no air conditioner. Therefore, as shown in Fig. 7, the lowest average temperature of the week occurs in the living room ( $26.2^{\circ}\text{C}$ ). There is no climate boundary between the dining room and the living room, so the average temperature of the dining room is also relatively low, at  $26.8^{\circ}\text{C}$ . In contrast, the temperatures of

the two bedrooms facing south and the bedroom in the northeast are higher. Due to the influence of air-conditioning, the daily temperature difference in the living room is the largest, while that in the northeast bedroom is the smallest.

### 2.3. Building energy retrofit strategies

The case building was newly built in 2017 and began to be occupied in 2018. At the time, its HVAC system and other building performance were in relatively good condition. However, there was an obvious temperature difference between the foam concrete part and the structural column on the inside of external wall due to the special and self-made structure without insulation material, leading to huge heat loss and extra energy demand. Therefore, one of the basic strategies to fill the gap was improving the holistic thermal performance of the building envelope. Considering what would have the least influence on household life, external thermal insulation, which can be installed onto the external surface totally from the outside, was adopted.



**Fig. 7.** The results of indoor temperature measurement during a typical week in summer.

**Table 3**

Supposed retrofit selections of external walls referred to in the local construction atlas.

Retrofit types	<i>i</i>	Insulation material	$\bar{D}_i$ (mm)	$\bar{U}_i$ (W/m <sup>2</sup> K)
Type A in Fig. 8	1	EPS panel	80	0.273
	2	PUR panel	65	0.254
	3	MPF panel	85	0.273
	4	Rock wool board	115	0.276
Type B in Fig. 8	5	Sprayed PUR rigid foam polyurethane	70	0.243
	6	EPS panel	120	0.241
	7	XPS panel	90	0.237
	8	PUR panel	70	0.251
	9	Rock wool board	130	0.265
Type C in Fig. 8	10	Rockwool board	130	0.289
	11	Vacuum insulation board	25	0.258
	12	Inorganic composite polystyrene board	130	0.299
	13	Polyphenylene plate	120	0.293
	14	PUR rigid foam polyurethane	70	0.273
	15	Graphite polystyrene board	90	0.286
	16	Graphite extrusion plate	80	0.260
	17	XPS panel	65	0.343

Since the outside layer of the original external wall was in the form of cast-in-site concrete, the retrofit strategies in this research possessed the common characteristic of cement-based external insulation methods, derived from the construction atlas published by the local government and divided into three main types. The construction details of three types of external wall retrofit methods are presented in Fig. 8. The specified wall selections with different insulation materials *i*, the upper limit of insulation material thickness  $\bar{D}_i$  (mm), and the final U-value of the external wall corresponding to the maximum thickness of insulation material  $\bar{U}_i$  (W/m<sup>2</sup> K) are illustrated in Table 3.

In terms of active energy-efficient retrofitting, crystalline silicon solar panels of 1.64 m<sup>2</sup> per piece were supposed to be installed on the pitched roof. This kind of panel has a high efficiency and low initial cost, which is suitable for the economic capacity of rural areas. The increase of solar panels follows the principle of preferentially setting them on the surface with the highest luminous efficiency. According to the amount of solar radiation received from different directions, the panels on the southern roof are supposed to be installed first, followed by the western and eastern. The household and possibly the contractor specified one product to be applied in this project. The energy generation per m<sup>2</sup> of roof and the maximum number of solar panels installed in different directions are presented in Table 4.

**Table 4**

Maximum amount of electricity generation by solar panels installed on each direction of the roof.

<i>j</i>		$A_j^{roof}$ (m <sup>2</sup> )	$E_j^{PV}$ (kWh/m <sup>2</sup> roof)	$\bar{N}_j^{PV}$	$\bar{P}_j^{PV}$ (kWp)
1	South	19.7	170.4	12	3.5
2	West	36.2	157.2	22	6.5
3	East	30.9	142.4	18	5.3

Note:  $A_j^{roof}$  represents the roof area of *j*-direction suitable for solar panel installation (m<sup>2</sup>);  $E_j^{PV}$  is the energy generation per m<sup>2</sup> of roof of *j*-direction (kWh/m<sup>2</sup> roof);  $\bar{N}_j^{PV}$  is the maximum number of solar panels installed on *j*-direction roof;  $\bar{P}_j^{PV}$  is the maximum peak power obtained by the panels installed on *j*-direction roof (kWp).

## 2.4. Optimization problem

Design optimization is the process through which design alternatives and their foreseen performance are evaluated against a set of criteria to determine the most appropriate design alternatives (Roberts et al., 2020). As stated before, insulation materials were considered to be added to the external walls, and solar panels were considered to be installed on the roof in this research. The optimization problem of selecting the best solution is described in the following paragraphs.

### 2.4.1. Design variables

In the design of the envelope retrofitting, two parameters, namely retrofit selection for the external wall and the thickness of insulation material, were used to identify the specific choice. Sets of envelope variables in this study were in the form of the following matrix:

$$X^{envelope} = \begin{pmatrix} X^{wall} \\ X^{thick} \end{pmatrix} \quad (1)$$

in which,  $X^{wall}$  and  $X^{thick}$  is the retrofit selection of the external wall and its corresponding thickness of the insulation material, which can be further represented in the following series:

$$X^{wall} = (x_1^{wall}, \dots, x_i^{wall}) \quad (2)$$

$$X^{thick} = (x_1^{thick}, \dots, x_i^{thick}) \quad (3)$$

On the other hand, the active energy saving system, the photovoltaic power generation equipment, was used to avoid disproportionate increase of cost when seeking the annual energy-balance target. Results of this part were shown in the form matrix as well:

$$X^{equipment} = \begin{pmatrix} X^{PV} \\ X^{number} \end{pmatrix} \quad (4)$$

in which,  $X^{PV}$  and  $X^{number}$  are the installed direction and number of solar panels, respectively, and they can be further represented in the series below:

$$X^{PV} = (x_1^{PV}, \dots, x_j^{PV}) \quad (5)$$

$$X^{num} = (x_1^{num}, \dots, x_j^{num}) \quad (6)$$

Since the results of these two retrofitting directions can be transformed into a unified form, a combined matrix named retrofitting-plans-set was generated as below:

$$X^{plan} = \begin{bmatrix} X^{wall}(x_1^{wall}, \dots, x_i^{wall}) & X^{thick}(x_1^{thick}, \dots, x_i^{thick}) \\ X^{PV}(x_1^{PV}, \dots, x_j^{PV}) & X^{num}(x_1^{num}, \dots, x_j^{num}) \end{bmatrix} \quad (7)$$

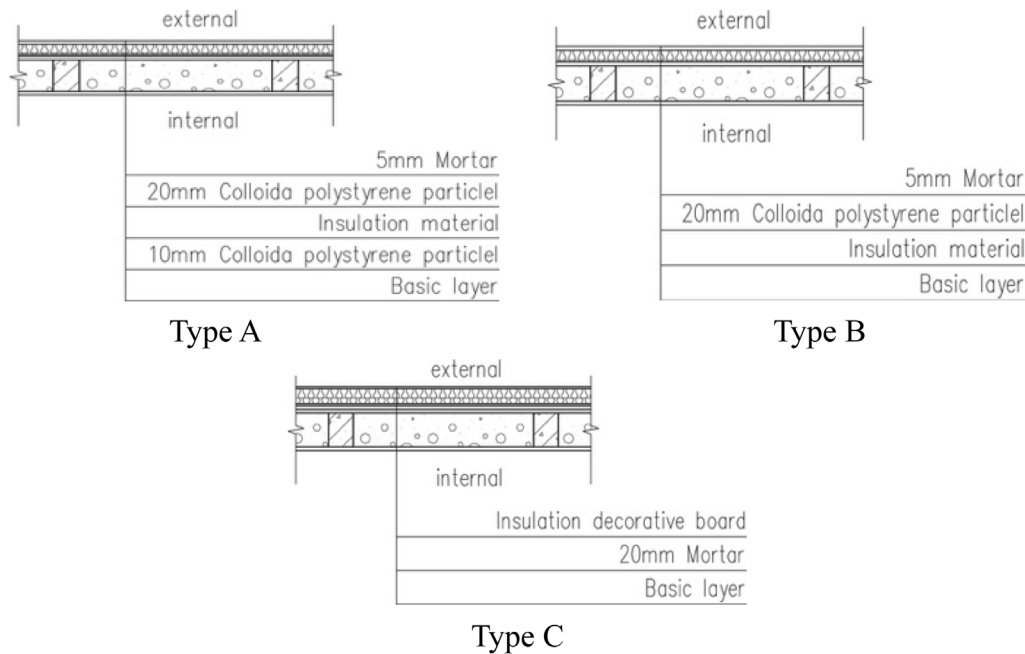


**Fig. 8.** The construction details of wall retrofit with external insulation installed.

#### 2.4.2. Objectives

The basic requirement of the retrofit strategy in this study was achieving a balance between the annual electricity generation from the rooftop PV system and the energy consumption after envelope retrofitting. Variables in the matrix  $X^{plan}$  automatically generate a huge number of different alternatives. As an energy-efficient retrofit project, there is no doubt that the amount of energy-saving after the envelope retrofit is an important indicator of the selection solution. The energy-saving performance after the external wall retrofitting was calculated by the following equation:

$$ES_{wall} = \frac{ES_{pre} - ES_{post}}{ES_{pre}} \times 100\% \quad (8)$$

where  $ES_{pre}$  and  $ES_{post}$  are annual building energy consumption before and after the retrofitting (kWh/year).

Taking into account the rural economic levels, in order to improve the attractiveness of retrofitting strategies to decision-makers, another indicator, the economic performance, was adopted as a main evaluating criterion in the optimization process, which could help judge the strategies more objectively and quantitatively. The reason comes not only from its own effectiveness but also from it being one of most significant factors when implementing the plan practically. The economic objectives considered in this study include minimizing the retrofit cost and shortening the payback period. The retrofit cost was calculated through a quota method, which contains that of the wall retrofitting and PV system installation as follows:

$$C_{tot} = C_{tot}^{wall} + C_{tot}^{PV} \quad (9)$$

where

$$C_{tot}^{wall} = A_{wall} \times C_i^{wall} \quad (10)$$

$$C_i^{wall} = (C_i^P + C_i^m + C_i^e) + (C_{d_i}^P + C_{d_i}^m + C_{d_i}^e) \times (x_i^{thick} - D_i^s)/d_i \quad (11)$$

$$C_{tot}^{PV} = \sum_{j=1}^J x_j^{num} \times C_0^{PV} \quad (12)$$

In Eqs. (7)–(10),  $C_{tot}$ ,  $C_{tot}^{wall}$ , and  $C_{tot}^{PV}$  are the total cost of the retrofit strategy, the cost of the wall retrofit, and the cost of the rooftop PV system installation, respectively.  $A_{wall}$  is the area of the retrofitted external walls ( $m^2$ ).  $C_i^P$ ,  $C_i^m$ , and  $C_i^e$  are the unit personal, material, and equipment prices of the wall retrofitting when adopting the  $i$ th wall selection with a standard thickness of the insulation material respectively (RMB/ $m^2$ ).  $D_i^s$  is the standard insulation material thickness of the  $i$ th wall selection (mm).  $C_{d_i}^P$ ,  $C_{d_i}^m$ , and  $C_{d_i}^e$  are the cost differences of personal, material, and equipment when the thickness of  $i$ th wall selection decreases  $d_i$  mm respectively (RMB/ $m^2$ ).  $C_0^{PV}$  is the unit cost of the solar panel, including the inverter, support, circuit, installment, and design fees (RMB).

The payback period  $T_p$  (year) is an important indicator to illustrate how fast the retrofit cost can be recouped and when it will start generating profit. It was calculated according to the following equation:

$$T_p = \frac{C_{tot}}{(ES_{pre} - ES_{post}) \times p_e + ES_{PV} \times p_s} \quad (13)$$

where  $ES_{PV}$  is the annual energy generation of PV system (kWh/year);  $p_e$  and  $p_s$  are the local electricity price for residents and revenue of the household PV system (RMB/kWh).

#### 2.4.3. Constraints

In this study, the purpose of the retrofit project was to meet the annual energy balance through external wall modification and rooftop PV system installation. The optimization of the retrofit solution is aimed at maximum energy savings, minimum retrofit cost, and the shortest payback period. During the optimization process, there were some logical, technical, and physical constraints concerning the design variables, their relationship, and the retrofit requirements, which needed to be incorporated into the optimization problem and are given as follows:

$$ES_{post} \leq ES_{PV} \quad (14)$$

$$\sum_{i=1}^I x_i^{wall} = 1, \text{for } x_i^{wall} \in \{0, 1\}, \forall i \in \{1, 2, \dots, I\} \quad (15)$$

$$x_i^{thick} \leq \bar{D}_i \quad (16)$$

$$\sum_{j=1}^J x_j^{PV} \geq 1, \text{ for } x_j^{PV} \in \{0, 1\}, \forall j \in \{1, 2, \dots, J\} \quad (17)$$

$$x_j^{num} \leq \overline{N_j^{PV}} \quad (18)$$

Inequality (14) is the basic requirement for all the retrofit strategies that the annual building energy consumption should be less than the energy generated by the rooftop PV system. Eq. (15) means that only one wall alternative can be applied in each retrofit strategy. There are 17 alternative wall alternatives in this study, all of which are derived from the construction atlas of Shandong Province (see Table 3). Inequality (16) illustrates that the insulation material thickness of the wall selection should be no more than the maximum thickness specified in the official construction atlas in Table 3. For calculating the practical circumstance, the insulation material thickness is divided into 10 mm for each simulation to calculate the amount of energy savings. Inequalities (17) and (18) illustrate that solar panels must be installed on at least one direction of roof and the number of the panels installed on the  $j$ -direction roof should be no more than the maximum number of panels presented in Table 4, respectively. Based on the optimization problem formulated above, the energy model will be used to simulate all possible scenarios, including wall retrofitting and solar panel installation, to find the optimal solution.

### 3. Results

#### 3.1. Model evaluation

Through the statistical analysis of the field measurement results and user surveys, several input parameters were calibrated, ranging from the operation schedule to the heating and cooling setpoint, as well as the natural ventilation schedule. Temperature data and actual electricity bills were monitored to calibrate the indoor temperature and energy consumption of the energy-simulation model. Table 5 illustrates the differences between the actual and simulated indoor temperature of each room during the two-month monitoring period. It can clearly be seen that the error rate of monitored rooms were all controlled under 10%.

Dots of blue and orange in Fig. 9 represent the ratio between the actual and simulated hourly temperature data during the winter and summer test periods. 45° trend lines in the figure represent a correspondence of 100%, and others represent that of 80%. It can be seen that the data is mainly distributed in the error range of  $\pm 20\%$ . As for the calibration of energy consumption, the actual energy use in 2019 was 7415.8 kWh, and the annual simulated energy consumption was 53.9 kWh/(m<sup>2</sup> year). The error rate between actual and simulated value was 8.3%. Therefore, the energy-simulation model was considered to be reliable, and retrofit strategies were applied to assess the economic and technical effects.

It is noted in Table 5 that the error rate in the winter testing period was lower than that in summer, which stems from different HVAC settings. The heating system was established strictly according to the actual situation and was in operation 24 h. In summer, the entire building was cooled by the only air conditioning in the living room. The doors of every bedroom were open, and a relatively open indoor environment was created. However, since the air conditioning was manually controlled by occupants, the operating schedule was not strictly conducted like the heating system. Factors such as user comfort, personal schedule, and other factors can cause temporary changes to the operation schedule. During the survey, occupants admitted that they sometimes might close the doors of some rooms in the

**Table 5**

Difference between the actual and simulated indoor temperature of each room during the monitoring months.

Location	Error rate between actual and simulated temperature (%)	
	Winter test period (Feb. 1st–Feb. 28th)	Summer test period (Aug. 13th–Sept. 12th)
Living room	8.22	9.34
Dining room	7.29	9.20
Master bedroom	5.11	9.44
Southeast bedroom	6.66	9.19
Northeast bedroom	5.72	9.12
Northwest bedroom	7.10	9.92

hope of saving electricity bills, but this behavior was completely random. These user behaviors led to a generally higher error rate of the simulation values of indoor temperature in summer testing period than in winter. This difference was also shown in Fig. 9, in which a wider vertical distribution (simulation values) in the summer was observed. The distribution of dots also reflects the effects of the air-conditioning system in the software. The simulation values of rooms with air conditioning system tends to be more stable than actual ones. It was represented by the apparent horizontal aggregation, which can be seen in the distribution of blue dots in all rooms and orange dots in the living room. It is observed that the minimum temperature of approximately 20 °C in winter was maintained according to the simulation results. It was hard to achieve in practice, although the distribution of values of the dining room and living room was in line with that situation to some extent. Reasons may stem from the un-reflected distribution of temperature difference in the heating pipe. The dining room and living room were located upstream of the heating system. The temperature of heating water dropped to a relatively low level after heating these areas. Therefore, the temperature difference in the pipe was inhomogeneous, which further led to the difference in the heat supply. Although a total temperature difference was set in the model, the simulation results were not entirely consistent with actual conditions according to the actual setting. This situation was more obvious in the area located downstream of the heating system than upstream.

#### 3.2. Retrofitting plan

According to the wall selections provided in Section 2.3, a total of three external thermal insulation systems with 4, 5, and 8 kinds of insulation material were selected for the envelope parameter, and they formed 17 different values for the final value of the retrofitted external wall  $X^{wall}$ . The thickness of the insulation board  $X^{thick}$  was originally a consistent variable, which means numerous possible values can be determined under its limitations. However, considering the dimension control and feasibility in practical construction, value ranges were divided every 10 mm from 0 to the upper limit of the insulation board in each wall selection.

According to the research of Fan and Xia (2017), with a given energy-efficiency target, the most economical transformation plan gives priority to retrofitting the envelope components. Therefore, a retrofitting plan with the greatest envelope thermal performance was considered to be the most economical choice at the same time. The regulation was proven through calculating all possible retrofitting methods that adopted the first wall selection ( $i = 1$ ); the results are listed in Table 6. When meeting the requirement of annual energy balance, the budget fluctuated between 44,459RMB (\$6669) and 43,082RMB (\$6462). The change of installed capacity of a PV system is not a continuous curve because the numbers of solar panels are integers. Therefore, as can

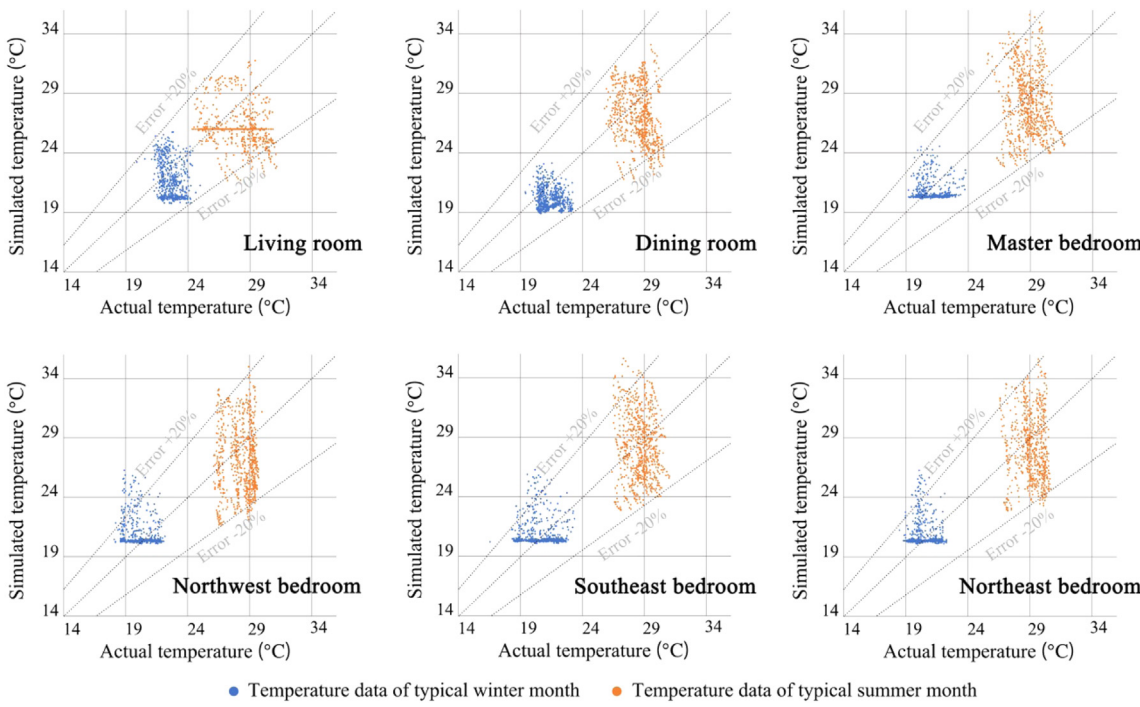


**Fig. 9.** Comparison of actual and simulated indoor temperature of each room during the monitoring months. (For interpretation of the references to color in this figure legend, the reader is referred to the web version of this article.)

be seen in Fig. 10, within the reasonable value of the insulation layer thickness, a proportional relationship between the budget and the thickness of insulation material was hard to observe. For example, when the thickness rises from 20 mm to 50 mm, the amount of installed capacity remains stable at 6.5 kWp. This situation stems from the fact that the energy saved by increasing the thickness was not sufficient to reduce one solar panel in the system. As a result, the improvement of thermal performance was reflected in the decrease of annual energy consumption rather than the decrease of the budget. By contrast, the total cost of the retrofitting plan rises with the increase of the thickness of insulation materials when the amount of installed capacity of the PV system stays unchanged. Therefore, with a given amount of installed capacity, the strategy with the lowest budget appears when the material thickness reaches its minimum value.

Taking the strategies with thicknesses of 60 mm, 20 mm, and 0 mm into consideration, the budget rose from 43,082RMB (\$6462) to 44,127RMB (\$6619). This regulation corresponds with that reported by Fan and Xia (2017), which means that the optimal plan with the lowest budget was predicted to be achieved when adopting the minimum number of solar panels and the thinnest insulation thickness under corresponding conditions. Based on this, all methods that have the potential to be the cheapest strategy are stated in Table 7. The wall selections reflect the choices of insulation layer presented in Table 3.

Even the regulation stated before shows the relationship between the thickness of insulation material and the total retrofitting cost. It was observed that the optimal retrofitting plan was not simply to adopt the thickest insulation material; rather, a relatively big value was used. It is interesting to note that the optimal peak power of the PV system fluctuates around 6.2 kWp. This fact reflects that when adopting the upper limit of insulation material as its thickness, the energy-saving potential of each plan stays similar. According to the research of Yu et al. (2016), the increase of cost is not proportional to the improvement of system performance. When the thermal performance of a certain retrofitting plan, especially the wall thermal insulation material,

**Table 6**

The energy saving rate and total retrofit cost corresponding to the different insulation material thickness in the case of the first wall selection ( $i = 1$ ).

$D_1$	$D_1^a$ (mm)	$P_1$ (kWp)	$ES_{post}$ (kWh/m <sup>2</sup> )	$ES_{PV}$ (kWh/m <sup>2</sup> )	$ES_{wall}$ (%)	$C_{tot}$ (RMB/\$)
80	80	6.2	44.0	45.0	18.3	43,748/6562
	70	6.2	44.3	45.0	17.7	43,415/6512
	60	6.2	44.7	45.0	17.0	43,082/6462
	50	6.5	45.1	47.0	16.2	44,270/6641
	40	6.5	45.6	47.0	15.3	43,937/6591
	30	6.5	46.2	47.0	14.2	43,605/6541
	20	6.5	46.9	47.0	12.9	43,272/6491
	10	6.5	47.9	49.1	11.1	44,459/6669
	0	6.5	49.1	49.1	8.9	44,127/6619

reaches a certain threshold value, the significantly increased capital investment can only obtain a little performance improvement. Therefore, in the industry standard, the optimal insulation effect tends to be the same. Although a retrofit method with better thermal performance can be obtained through customization during the implementation of the scheme, the procurement of non-standard insulation materials will cause a significant increase in the construction cost, so it was not used in this study.

Under the premise of meeting the annual energy balance, one cost-optimal plan was selected from each wall selection with the corresponding insulation thickness and peak power of the PV system, as shown in Table 7. Generally, 16.6%–20.9% of building energy consumption can be reduced through these wall retrofits. The peak power of the PV system basically stabilizes at 6.2 kWp. Selections 9 and 10 had a better passive energy-saving performance, with only 5.9 kWp of peak power required to balance building energy consumption throughout the year.

Fig. 11 gives information on the economic performance of each retrofit plan: the relationship between the total retrofitting investment and its payback period. A trend line with a slope of approximately 0.28 was observed, which means that the payback period increased linearly with the increase in investment and 0.28-year was taken by each 1000 RMB investment to payback.

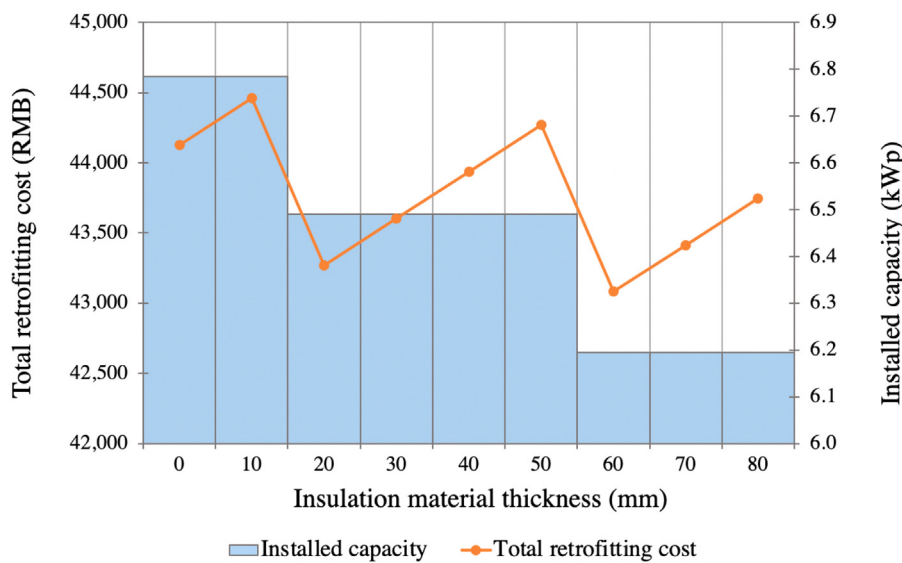


**Fig. 10.** Relationship between the insulation material thickness, total retrofitting cost, and the installed capacity of PV system adopting the first wall selection ( $i = 1$ ).

**Table 7**

The lowest cost plan in each wall selection retrofit set and its corresponding insulation thickness.

$i$	$x_i^{thick}$ (mm)	$P_i$ (kWp)	$ES_{post}$ (kWh/m <sup>2</sup> )	$ES_{PV}$ (kWh/m <sup>2</sup> )	$ES_{wall}$ (%)	$C_{tot}$ (RMB/\$)	$T_p$ (year)
1	60	6.2	44.7	45.0	17.0	43,082/6462	11.1
2	40	6.2	44.6	45.0	17.2	43,415/6512	11.1
3	50	6.2	44.8	45.0	16.8	42,869/6430	11.0
4	60	6.2	45.0	45.0	16.6	42,703/6405	11.0
5	40	6.2	44.8	45.0	16.8	44,593/6689	11.5
6	60	6.2	44.6	45.0	17.1	42,082/6312	10.8
7	70	6.2	44.9	45.0	16.7	43,579/6537	11.2
8	40	6.2	44.9	45.0	16.6	42,415/6362	10.9
9	130	5.9	42.9	42.9	20.5	41,578/6237	10.7
10	130	5.9	42.6	42.9	20.9	43,371/6506	11.2
11	20	6.2	44.4	45.0	17.6	45,918/6888	11.7
12	90	6.2	44.6	45.0	17.2	44,445/6667	11.4
13	80	6.2	44.8	45.0	16.9	44,540/6681	11.4
14	50	6.2	44.6	45.0	17.2	45,604/6841	11.7
15	60	6.2	44.9	45.0	16.7	43,804/6571	11.3
16	50	6.2	44.9	45.0	16.7	43,590/6539	11.2
17	60	6.2	44.6	45.0	17.3	44,873/6731	11.5

The best economic performance was observed in Selections 6, 8, and 9, among which the total costs were no more than 42.5 kRMB. Selection 9 had the shortest payback period (10.7 years), followed by Selection 6 (10.8 years) and Selection 8 (10.9 years). Fig. 12 illustrates the environmental and economic performance of each retrofit plan simultaneously. The annual energy consumption was approximately 44.7 kWh/m<sup>2</sup>. While that of selections 9 and 10 was obviously lower which is less than 43 kWh/m<sup>2</sup>. It shows that applying retrofit Selections 9 and 10 led to a significantly lower energy consumption, the energy savings of which were 20.5% and 20.9%, respectively. Retrofitting using Selection 9 also shows a great economic advantage in both retrofitting cost and payback period. After comprehensive evaluation of both environmental and economic effects, Selection 9 was considered to be the optimal choice of all possible strategies. Overall, the results obtained in the case study verify the effectiveness of the proposed model in improving the energy efficiency of existing buildings, making the best use of investment by means of optimally determining a retrofitting strategy for the building.

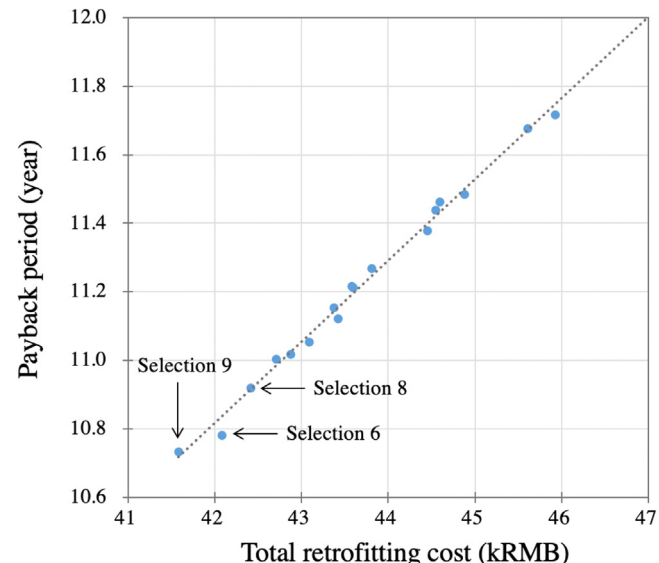


**Fig. 11.** Relationship between total retrofitting cost and payback period adopting each retrofitting set.

#### 4. Discussion

Inferred from results, rock wool, under the existing construction conditions, tended to have the highest cost performance. Firstly, the construction cost with rock wool as insulation material was lower than the others when seeking a similar thermal performance. When the type B of the wall retrofit system was selected, and 45 kWh/m<sup>2</sup> of the annual energy generation was obtained by the PV system, the thickness of rock wool board was 70 mm with a unit cost at 823.71 RMB/10 m<sup>2</sup>. These values were 80 mm and 994.14 RMB/10 m<sup>2</sup> when selecting type C. They were both the lowest unit price within their construction methods. Secondly, the construction of rock wool tended to be the most skilled. Selections 9 and 10, which were the only two that could keep the annual energy consumption lower than 42.9 kWh/m<sup>2</sup>, both took rock wool as insulation material. This conclusion was consistent with current Chinese industry tendencies. According

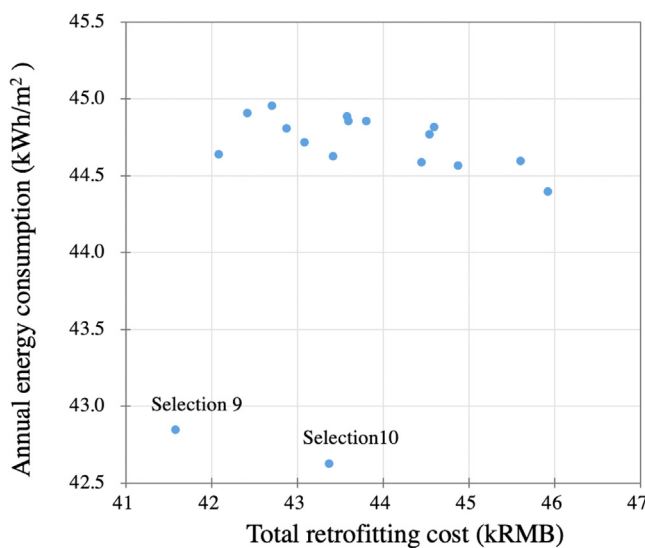


**Fig. 12.** Relationship between total retrofitting cost and annual energy consumption adopting each retrofitting set.

to “Code of Design on Building Fire Protection and Prevention (GB 50016-2014)” ([Ministry of Housing and Urban-Rural Development of the People’s Republic of China, 2015](#)), the insulation material of envelopes needs to be non-flammable, and flame retardant material, such as XPS and EPS, can only be adopted under strict limits. It prevents the use of XPS and EPS in urban areas, although it can still be used in some rural places like Jining. The effect was reflected in advantages of both price and performance of rock wool, as shown in the results.

Building energy simulation is an important and efficient tool to evaluate the retrofitting strategies, which helps set an applicable target and make the tradeoff between cost and performance. Given the construction particularity and irregularity of rural dwellings, detailed construction is no doubt greatly significant. However, on one hand, rural residences are rarely built with detailed drawings. The thermal performance can hardly be reflected through merely geometric information. On the other hand, local builders tend to construct according to their engineering experience, rather than the united standard code. Building components are, therefore, hard to reflect with solutions in a prebuilt database. This study managed to obtain the thermal performance of target building through the on-site survey. A simulation model was then established and verified according to measured data. The comprehensive error was controlled to be less than 10% in the end. Accompanied by verifying the method feasibility, it calls for the recommendation to implement on-site measurement in the retrofit design of rural construction. Additionally, the construction method adopted in this study for those of envelope thermal performance, can be supplemented for the benchmark of local rural construction method. This study is a good sample of rural energy-efficient renovation, combined with envelope retrofitting and solar energy utilization. It also reflects the large application potential of the decentralized rooftop PV system in the vast rural areas. The selection process for the optimal solution provides specific implementation steps for balancing energy savings and retrofit costs. The calculation of the two indicators, retrofitting cost and payback period, helps householders have a more comprehensive understanding of the economic benefits and reduce their investment concerns. Also, this study provides a case for balancing the insulation layer thickness with the installed capacity of PV system for new rural houses in the future.

This study also yields some limitations, especially the selection range of the potential retrofitting plans. This study selected the passive and active retrofit method, only including wall reconstruction and rooftop PV system installation. However, more modification schemes for envelope components should be added to the potential sets in the future. Heat loss through doors and windows accounts for 20%–30% of the total heat loss of northern Chinese rural houses, so replacing doors and windows that have high heat transmission coefficient and poor airtightness can further reduce building energy consumption ([Ma et al., 2015](#)). Whether to install rooftop PV systems is to be determined according to local solar energy resources and is not generally applicable to all Chinese rural houses. For southern areas with insufficient solar energy resources, the payback period for the PV systems is relatively long, so the rational development of renewable energy such as biogas should be considered. Besides, the retrofit requirement was just set to meet the annual energy balance and select the environmentally and economically optimal retrofit strategy. Future improvement of this study could expand to more diverse choices of energy-saving requirements. Homeowners can choose to meet 80%, 75%, or 65% of the energy-saving rate according to their housing performance status and retrofit budget, as well as the local energy-efficient building standards. An increase in the number of solar panels installed can be further considered, where the surplus power can be sold to the grid to gain benefits. The payback periods under the two circumstances of the energy consumption balance and the surplus electricity selling can be compared for exploring other retrofit potentials.

## 5. Conclusion

This paper designed a practical energy-efficient retrofit process for Chinese rural houses built without the supervision of construction norms. A rural house in Shandong province was used for the case study. This self-built house has the common construction uncertainty and high energy consumption problem of Chinese rural housing. Both passive and active retrofit schemes were combined to achieve the annual energy balance, and one optimization model was established to select the optimal strategy considering environmental and economic factors simultaneously. This research emphasized considering of the actual application constraints when establishing the optimization model rather than conducting idealized numerical calculations.

The necessity of on-site measurement and user survey is more prominent in the energy-efficient retrofit of non-benchmarked houses, especially the thermal measurement of the external walls. Through field measurement, the specific location of the heat bridges and the heat transmission coefficient of each part of external walls were determined. Indoor temperature monitoring was conducted in winter and summer for one month, respectively. The results were combined with the actual electricity bill to calibrate the energy model within 10% error rate, which laid a solid foundation for the effective simulation of the subsequent retrofit methods. During the optimization process, the retrofit plan with rock wool as the insulation material stood out among the 17 wall selections, and when combined with 5.9 kWp of rooftop PV system, it can achieve 20.5% energy savings and the best economic benefits (41.6kRMB investment cost and 10.7-year payback period). It is noted that under the retrofit requirements set in this paper (meeting the annual energy balance), the cost-optimal plan appears to be a combination of the minimum-installed capacity of the PV system and the thinnest insulation layer thickness. However, the amount of energy savings at this time is not the maximum value. Continuing to increase the insulation material thickness could further reduce energy consumption but will increase the retrofit cost.

For rural houses with different performance situations, the energy savings and the retrofit costs could be different by applying the energy-efficient retrofit process proposed in this study. But this general process is still instructive for the energy-efficient retrofits of other buildings in different regions and different uses with uncertain performance. The research is expected to promote energy-efficient retrofit programs for Chinese rural houses to improve the comfort and living conditions of rural dwellers and to narrow the energy gap and inequality between urban and rural areas.

### Nomenclature

$A_j^{\text{roof}}$	Roof area of $j$ -direction suitable for solar panel installation ( $\text{m}^2$ )
$A_{\text{wall}}$	Area of the retrofitted external walls ( $\text{m}^2$ )
$D_i$	Upper limit of the $i$ th insulation material thickness (mm)
$C_i^p$	Unit labor price of the wall retrofitting when adopting the $i$ th wall selection with a standard thickness of the insulation material respectively (RMB/ $\text{m}^2$ )
$C_{d_i}^p$	Cost difference of labor when the thickness of $i$ th wall selection decreases $d_i$ mm respectively (RMB/ $\text{m}^2$ )
$C_i^m$	Unit material price of the wall retrofitting when adopting the $i$ th wall selection with a standard thickness of the insulation material respectively (RMB/ $\text{m}^2$ )
$C_{d_i}^m$	Cost difference of material when the thickness of $i$ th wall selection decreases $d_i$ mm respectively (RMB/ $\text{m}^2$ )
$C_i^e$	unit equipment price of the wall retrofitting when adopting the $i$ th wall selection with a standard thickness of the insulation material respectively (RMB/ $\text{m}^2$ )
$C_{d_i}^e$	Cost difference of equipment when the thickness of $i$ th wall selection decreases $d_i$ mm respectively (RMB/ $\text{m}^2$ )
$C_0^P$	Unit cost of the solar panel, including the inverter, support, circuit, installment, and design fees (RMB)
$C_{\text{tot}}^P$	Total cost of PV system installation (RMB)
$C_{\text{wall}}$	Total cost of wall retrofitting (RMB)
$C_{\text{tot}}$	Total cost of the retrofit plan (RMB)
$D_i^s$	Standard insulation material thickness of the $i$ th wall selection (mm)
$d_i$	Decreased thickness of the $i$ th wall selection (mm)
$E_j^P$	Energy generation per $\text{m}^2$ roof of $j$ -direction ( $\text{kWh}/\text{m}^2$ roof)
$ES_{\text{pre}}$	Annual building energy consumption before the retrofitting ( $\text{kWh}/\text{year}$ )
$ES_{\text{post}}$	Annual building energy consumption after the retrofitting ( $\text{kWh}/\text{year}$ )
$ES_{\text{PV}}$	Annual energy generation of PV system ( $\text{kWh}/\text{year}$ )
$ES_{\text{wall}}$	Ratio between the annual energy savings after the external wall retrofitting and the building energy consumption before the retrofitting (%)
$N_j^P$	Maximum number of solar panels installed on $j$ -direction roof
$P_j^P$	Maximum peak power obtained by the panels installed on $j$ -direction roof (kWp)
$p_e$	Local electricity price for residents (RMB/ $\text{kWh}$ )
$p_s$	Local revenue of household PV system (RMB/ $\text{kWh}$ )
$T_p$	Payback period (year)
$U_i$	Final U-value of the external wall with the maximum thickness of the $i$ th insulation material ( $\text{W}/\text{m}^2 \text{ K}$ )

### CRedit authorship contribution statement

**Xinyi Hu:** Conceptualization, Methodology, Investigation, Software, Validation, Writing - original draft. **Yiming Xiang:** Methodology, Investigation, Data Curation, Writing - original draft. **Hong Zhang:** Supervision, Funding acquisition. **Qi Lin:** Investigation. **Wei Wang:** Supervision, Writing - review & editing. **Haining Wang:** Funding acquisition.

### Declaration of competing interest

The authors declare that they have no known competing financial interests or personal relationships that could have appeared to influence the work reported in this paper.

### References

- Asase, S.R., Ugursal, V.I., Beausoleil-Morrison, I., 2017. Techno-economic feasibility evaluation of air to water heat pump retrofit in the Canadian housing stock. *Appl. Therm. Eng.* 111, 936–949. <http://dx.doi.org/10.1016/j.applthermaleng.2016.09.117>.
- Ascione, F., Bianco, N., Mauro, G.M., Napolitano, D.F., 2019. Retrofit of villas on mediterranean coastlines: Pareto optimization with a view to energy-efficiency and cost-effectiveness. *Appl. Energy* 254, <http://dx.doi.org/10.1016/j.apenergy.2019.113705>.
- Augenbroe, G., 2002. Trends in building simulation. *Build. Environ.* 37, 891–902. [http://dx.doi.org/10.1016/S0360-1323\(02\)00041-0](http://dx.doi.org/10.1016/S0360-1323(02)00041-0).
- Ayres, J.M., Stamper, E., 1995. Historical development of building energy calculations. *ASHRAE J.* 37, <https://www.osti.gov/biblio/37088> (accessed April 23, 2020).
- Bao, L., Zhao, J., Zhu, N., 2012. Analysis and proposal of implementation effects of heat metering and energy efficiency retrofit of existing residential buildings in northern heating areas of China in the 11th Five-Year Plan period. *Energy Policy* 45, 521–528. <http://dx.doi.org/10.1016/j.enpol.2012.02.065>.
- Becchio, C., Dabbene, P., Fabrizio, E., Monetti, V., Filippi, M., 2015. Cost optimality assessment of a single family house: Building and technical systems solutions for the nZEB target. *Energy Build.* 90, 173–187. <http://dx.doi.org/10.1016/j.enbuild.2014.12.050>.
- Casquero-Modrego, N., Goñi Modrego, M., 2019. Energy retrofit of an existing affordable building envelope in Spain, case study. *Sustainable Cities Soc.* 44, 395–405. <http://dx.doi.org/10.1016/j.scs.2018.09.034>.
- Chen, S., Guan, J., Levine, M.D., Xie, L., Yowargana, P., 2013. Elaboration of energy saving renovation measures for urban existing residential buildings in north China based on simulation and site investigations. *Buil. Simul.* 6, 113–125. <http://dx.doi.org/10.1007/s12273-013-0114-y>.
- China Building Energy Consumption Report 2019, 2019. China association of building energy efficiency. <https://fanneng.com/supplInfo/detail/3e501e9df6364fd190ac9bffe9d2718a>.
- China Weather Network, 2009. Climate characteristics of Jining city. <http://www.weather.com.cn/shi{and}ong/sdqh/gsqhtd/11/86239.shtml> (accessed January 14, 2021).
- Coakley, D., Raftery, P., Keane, M., 2014. A review of methods to match building energy simulation models to measured data. *Renew. Sustain. Energy Rev.* 37, 123–141. <http://dx.doi.org/10.1016/j.rser.2014.05.007>.
- Evans, M., Yu, S., Song, B., Deng, Q., Liu, J., Delgado, A., 2014. Building energy efficiency in rural China. *Energy Policy* 64, 243–251. <http://dx.doi.org/10.1016/j.enpol.2013.06.040>.
- Fan, Y., Xia, X., 2017. A multi-objective optimization model for energy-efficiency building envelope retrofitting plan with rooftop PV system installation and maintenance. *Appl. Energy* 189, 327–335. <http://dx.doi.org/10.1016/j.apenergy.2016.12.077>.
- Gupta, R., Gregg, M., 2016. Do deep low carbon domestic retrofits actually work? *Energy Build.* 129, 330–343. <http://dx.doi.org/10.1016/j.enbuild.2016.08.010>.
- He, B.J., Yang, L., Ye, M., 2014. Building energy efficiency in China rural areas: Situation, drawbacks, challenges, corresponding measures and policies. *Sustainable Cities Soc.* 11, 7–15. <http://dx.doi.org/10.1016/j.scs.2013.11.005>.
- Hinnells, M., 2008. Technologies to achieve demand reduction and microgeneration in buildings. *Energy Policy* 36, 4427–4433. <http://dx.doi.org/10.1016/j.enpol.2008.09.029>.
- Hong, T., Yang, L., Hill, D., Feng, W., 2014. Data and analytics to inform energy retrofit of high performance buildings. *Appl. Energy* 126, 90–106. <http://dx.doi.org/10.1016/j.apenergy.2014.03.052>.
- Li, F., Gao, X., Wang, Y., 2011. Regional differentiation of housing structure and its influencing factors in rural areas of China. *Prog. Geogr.* 30, 1555–1563.

- Li, N., Yang, Z., Becerik-Gerber, B., Tang, C., Chen, N., 2015. Why is the reliability of building simulation limited as a tool for evaluating energy conservation measures? *Appl. Energy* 159, 196–205. <http://dx.doi.org/10.1016/j.apenergy.2015.09.001>.
- Li, B., You, L., Zheng, M., Wang, Y., Wang, Z., 2020. Energy consumption pattern and indoor thermal environment of residential building in rural China. *Energy Buil. Environ.* 1, 327–336. <http://dx.doi.org/10.1016/j.enbenv.2020.04.004>.
- Liu, Y., Guo, W., 2013. Effects of energy conservation and emission reduction on energy efficiency retrofit for existing residence: A case from China. *Energy Build.* 61, 61–72. <http://dx.doi.org/10.1016/j.enbuild.2013.01.033>.
- Liu, Y., Liu, T., Ye, S., Liu, Y., 2018. Cost-benefit analysis for energy efficiency retrofit of existing buildings: A case study in China. *J. Cleaner Prod.* 177, 493–506. <http://dx.doi.org/10.1016/j.jclepro.2017.12.225>.
- Luddeni, G., Krarti, M., Pernigotto, G., Gasparella, A., 2018. An analysis methodology for large-scale deep energy retrofits of existing building stocks: Case study of the Italian office building. *Sustainable Cities Soc.* 41, 296–311. <http://dx.doi.org/10.1016/j.scs.2018.05.038>.
- Ma, L., Shao, N., Zhang, J., Zhao, T., 2015. The influence of doors and windows on the indoor temperature in rural house. In: *Procedia Engineering*. Elsevier Ltd, pp. 621–627. <http://dx.doi.org/10.1016/j.proeng.2015.08.1051>.
- Magrini, A., Magnani, L., Pernetti, R., 2014. Opaque building envelope. In: Magrini, A. (Ed.), *Building Refurbishment for Energy Performance: A Global Approach*. Springer International Publishing, Cham, pp. 1–59. [http://dx.doi.org/10.1007/978-3-319-03074-6\\_1](http://dx.doi.org/10.1007/978-3-319-03074-6_1).
- Manke, J., Hittle, D., Hancock, C., 1996. Calibrating building energy analysis models using short term test data. <https://www.osti.gov/biblio/438671> (accessed April 24, 2020).
- Mata, É., Sasic Kalagadis, A., Johnsson, F., 2013. Energy usage and technical potential for energy saving measures in the Swedish residential building stock. *Energy Policy* 55, 404–414. <http://dx.doi.org/10.1016/j.enpol.2012.12.023>.
- Ministry of Housing and Urban-Rural Development of the People's Republic of China, 2015. Code for fire protection design of buildings (GB 50016-2014). China Planning Press, Beijing.**
- Nihal, G., Aydinl̄p, M., Ugursal, V.I., 2018. Techno-economical analysis of building envelope and renewable energy technology retrofits to single family homes. *Energy Sustain. Dev.* 45, 159–170. <http://dx.doi.org/10.1016/j.esd.2018.06.006>.
- Pan, Y., Huang, Z., Wu, G., 2007. Calibrated building energy simulation and its application in a high-rise commercial building in Shanghai. *Energy Build.* 39, 651–657. <http://dx.doi.org/10.1016/j.enbuild.2006.09.013>.
- Pedrini, A., Westphal, F.S., Lamberts, R., 2002. A methodology for building energy modelling and calibration in warm climates. *Build. Environ.* 37, 903–912. [http://dx.doi.org/10.1016/S0360-1323\(02\)00051-3](http://dx.doi.org/10.1016/S0360-1323(02)00051-3).
- Qi, F., Cui, F., Lv, W., Zhang, T., Musonda, B.M., 2019. Regional similarity of shape coefficient of rural residences—Taking hangzhou rural region as a case. *Buil. Simul.* 12, 597–604. <http://dx.doi.org/10.1007/s12273-019-0515-7>.
- Roberts, M., Allen, S., Coley, D., 2020. Life cycle assessment in the building design process – A systematic literature review. *Build. Environ.* 185, 107274. <http://dx.doi.org/10.1016/j.buildenv.2020.107274>.
- Rosso, F., Ciancio, V., Dell'Olmo, J., Salata, F., 2020. Multi-objective optimization of building retrofit in the mediterranean climate by means of genetic algorithm application. *Energy Build.* 216, 109945. <http://dx.doi.org/10.1016/j.enbuild.2020.109945>.
- Song, B., Deng, Q., 2018. *Technology for present situation and prospect of energy rural construction. District Heat.* 05, 111–116.
- Suárez, R., Fernández-Agüera, J., 2015. Passive energy strategies in the retrofitting of the residential sector: A practical case study in dry hot climate. *Buil. Simul.* 8, 593–602. <http://dx.doi.org/10.1007/s12273-015-0234-7>.
- Taheri, M., Tahmasebi, F., Mahdavi, A., 2013. A case study of optimization-aided thermal building performance simulation calibration, in: 13th Conference of International Building Performance Simulation Association, Chambéry, France, 2013, pp. 603–607, <https://pdfs.semanticscholar.org/2f21/266c9e22c7720949b7cb281618e895d32eae.pdf> (accessed April 24, 2020).
- Tahsildoust, M., Zomorodian, Z.S., 2020. Energy, carbon, and cost analysis of rural housing retrofit in different climates. *J. Buil. Eng.* 30, 101277. <http://dx.doi.org/10.1016/j.jobc.2020.101277>.
- Xin, L., Chenchen, W., Chuanzhi, L., Guohui, F., Zekai, Y., Zonghan, L., 2018. Effect of the energy-saving retrofit on the existing residential buildings in the typical city in northern China. *Energy Build.* 177, 154–172.
- Yang, X., Jiang, Y., Yang, M., Shan, M., 2010. Energy and environment in chinese rural housing: Current status and future perspective. *Front. Energy Power Eng. China* 4, 35–46. <http://dx.doi.org/10.1007/s11708-010-0001-5>.
- Yang, T., Pan, Y., Mao, J., Wang, Y., Huang, Z., 2016. An automated optimization method for calibrating building energy simulation models with measured data: Orientation and a case study. *Appl. Energy* 179, 1220–1231. <http://dx.doi.org/10.1016/j.apenergy.2016.07.084>.
- Yu, Z.J., Chen, J., Sun, Y., Zhang, G., 2016. A GA-based system sizing method for net-zero energy buildings considering multi-criteria performance requirements under parameter uncertainties. *Energy Build.* 129, 524–534. <http://dx.doi.org/10.1016/j.enbuild.2016.08.032>.
- Zhang, L., Yang, Z., Chen, B., Chen, G., 2009. Rural energy in China: Pattern and policy. *Renew. Energy* 34, 2813–2823. <http://dx.doi.org/10.1016/j.renene.2009.04.006>.
- Zhou, L., Li, J., Chiang, Y.H., 2013. Promoting energy efficient building in China through clean development mechanism. *Energy Policy* 57, 338–346. <http://dx.doi.org/10.1016/j.enpol.2013.02.001>.